Toward a Theory of Coherent Synchrotron Radiation in Realistic Vacuum Chambers

R. Warnock, SLAC National Accelerator Laboratory and
Dept. of Mathematics and Statistics, U. of New Mexico

Sincere thanks to Jack Bergstrom, David Bizzozero, and Chris Mayes.

September 19, 2017

ABSTRACT

The effort to understand CSR in whispering gallery modes has led to a general scheme for studying fields in a rectangular chamber of varying width. It works in the frequency domain, with Fourier development only in the vertical coordinate. The calculation reduces to integration of a simple system of ordinary differential equations, with arc length s as the independent variable. A new scheme to handle a singular or highly concentrated charge/current is an essential feature. An implicit integration rule appears to avoid the approximation of slowly varying amplitude. The time for the field calculation is so short that it will be negligible compared to that for charge/current construction and particle pushing in a self-consistent macroparticle simulation, which could be in three dimensions.

Whispering Gallery Modes

Fields excited by a bunch circulating in a smooth torus of constant rectangular cross-section can be calculated in terms of high order Bessel functions, including effects of wall resistance.

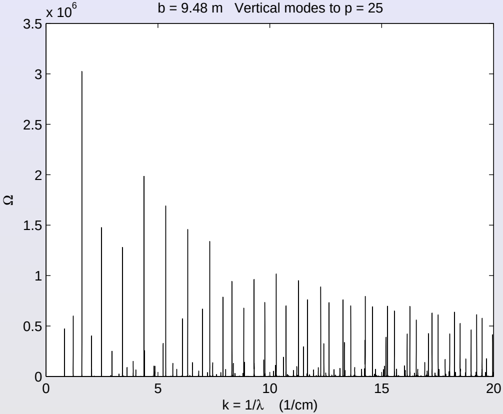

Figure: $\mathrm{Re}\ Z(n, n\omega_0)$ for parameters of VUV light source, vs. wave number $1/\lambda$ in units of cm^{-1}.

Experimental Spectra

Spectrum of CSR measured at NSLS-VUV (BNL) in 2001, by an interferometer and and also by microwave techniques.

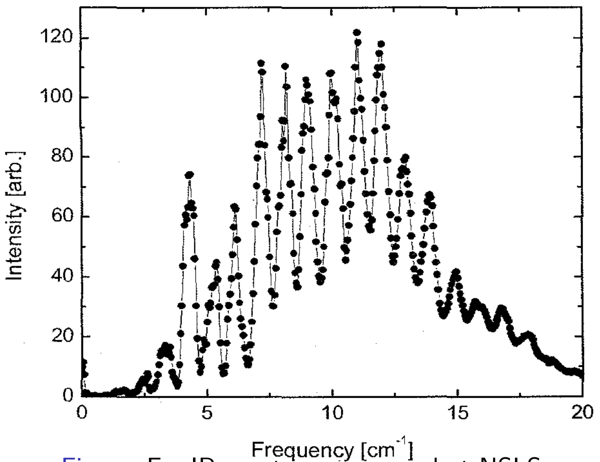

Figure: Far IR spectrum measured at NSLS

Table: Theoretical frequencies compared to data from VUV

Exp.	**Thy.**	**Exp.**	**Thy.**
0.80	0.827	6.10	6.31
0.93	—	7.25	7.32
1.32	1.21	9.00	8.32
1.57	1.60	10.0	9.29
2.10*	2.04	11.1	10.28
2.40	2.48	12.0	11.29
2.76*	2.94	12.8	12.33
3.10*	3.26	13.8	13.31
3.66*	3.62	15.0	14.3
3.88*	3.90	15.7-15.9	15.3
4.20	4.38	16.7	16.3
5.25	5.34	18.0	17.3
		18.8*	18.3

IR Vacuum Chamber at the Canadian Light Source

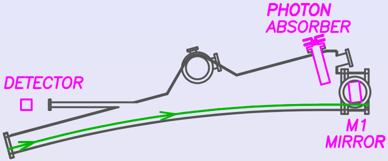

Figure: Fluted vacuum chamber at the FIR dipole with bending radius $R = 7.143$ m and deflection angle $\theta = 15^\circ$. The maximum excursion of the outer wall from the beam (——) is 33 cm.

Experiments: (a) diode detector, sees radiation reflected backward from photon absorber and mirror support assembly. (b) signal picked up by M1 mirror, sent to long interferometer (resolution to $\Delta k = 0.0009\mathrm{cm}^{-1}$.).

CSR spectrum at CLS

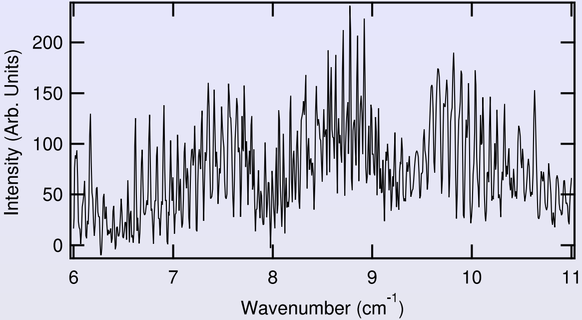

Figure: Peak spacing $\Delta k = \Delta\lambda^{-1} = 0.074\mathrm{cm}^{-1}$.

Position of peaks extremely stable over *years*, and independent of machine set-up (current, energy, bunch length, number of bunches, etc.) *and* IR beamline hardware.

CLS spectrum and whispering gallery theory

To fit the peak spacing of $\Delta k = 0.074\mathrm{cm}^{-1}$ with the toroidal model, the distance from the beam to the outer wall in the model has to be 33 cm, equal to the maximum distance in the flared chamber.

In a perturbative theory, treating the lowest order effect of a wall excursion, this is explained qualitatively (to be published). A distinctly local short wave length oscillation builds up in the region of the flare, making peaks in the spectrum that are not the whispering gallery modes of the full toroidal chamber. A more quantitative calculation of the spectrum is one goal of the effort described in this talk.

Direct observation of CSR wake fields in the flared chamber

Although we have not yet understood the interferometer data extending to the THz, we have simulated major features of the signal in the backward diode detector (35-110 GHz). This by a time domain integration of the Maxwell curl equations in curvilinear coordinates (after FT in the vertical coordinate). (Bizzozero's thesis at UNM, discontinuous Galerkin method, PRL **114**, 204801 (2015))

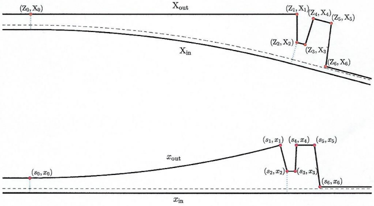

Figure 5.1: Physical laboratory frame (top) and Frenet-Serret transformed frame (bottom). The dashed line indicates the source's trajectory, the region between the dotted blue lines indicate where the curvature is non-zero, and the red dots indicate points where the boundary geometry transitions.

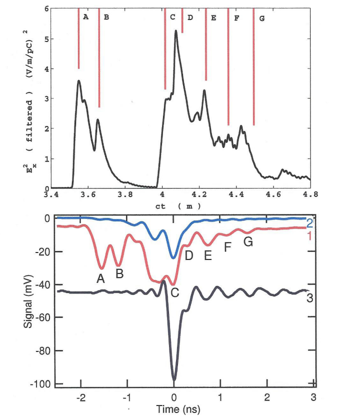

Figure: Upper graph shows simulated diode signal, with peaks correlated to experimental peaks A-G (red curve in lower graph)

The distance A-B to the first wake pulse is 12cm, close to the 13.5cm spacing of lines in the interferogram, the reciprocal of the spacing 0.074 cm^{-1} of the frequency spectrum.

Calculated field pattern in flared chamber

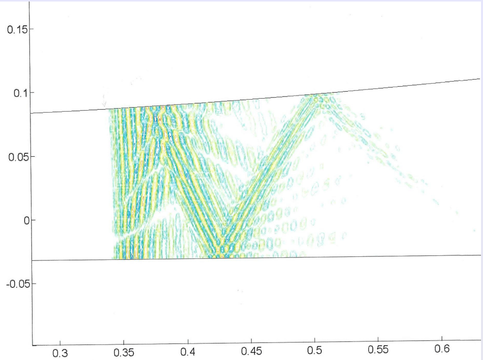

Figure: E_z at entrance to backword port. Source is ribbon line charge with 2mm Gaussian bunch form.

Fine detail displayed in a sophisticated finite element method – discontinuous Galerkin. Drawback: expensive for very short driving bunch. Hard to get high frequency spectrum.

Five Star (*****) Computational Method

Use standard accelerator (Frenet-Serret) coordinates (s, x, y), with reference trajectory in plane $y = 0$ consisting of bends and straights in arbitrary sequence. Rectangular chamber with top and bottom plates at $y = \pm g$, inner and outer sidewalls at $x = x_-(s)$ and $x_+(s)$. Perfectly conducting, to start.

All field and charge/current components represented as

$$f(s, x, y, t) = \sum_{p=0}^{\infty} \int_{-\infty}^{\infty} dk e^{ik(s-\beta ct)} \varphi_p(y) \hat{f}_p(s, x, k) \;, \qquad (1)$$

where the vertical Fourier mode φ_p is chosen to meet boundary conditions at $y = \pm g$

Think of (1) as the FT with respect to beam frame coordinate $s - \beta ct$ at fixed s. The representation is general, but contains primarily right-moving waves if and only if $\hat{f}(s, x, k)$ is slowly varying in s.

Two independent wave equations determine all fields

All field components are expressed in terms of $\hat{E}_{yp}$ and $\hat{H}_{yp}$ and their derivatives w.r.t. x and s. Moreover, $\hat{E}_{yp}$ and $\hat{H}_{yp}$ are determined by independent wave equations, not coupled even by boundary conditions (for perfect conductors). Within a bend of radius ρ,

$$\frac{\partial^2 u}{\partial s^2} + 2ik\frac{\partial u}{\partial s} =$$
$$-\left(\frac{x+\rho}{\rho}\right)^2\left[\frac{\partial^2 u}{\partial x^2} + \frac{1}{x+\rho}\frac{\partial u}{\partial x} + \left(\gamma_p^2 - \left(\frac{k\rho}{x+\rho}\right)^2\right)u - S\right],$$

$$\gamma_p^2 = k^2 - \alpha_p^2 \,, \quad \alpha_p = \pi p/2g \,. \tag{2}$$

Slowly varying amplitude approximation (SVA, paraxial approx.):

$$\left\|\frac{\partial^2 u}{\partial s^2}\right\| \ll 2k\left\|\frac{\partial u}{\partial s}\right\| \,, \quad k > k_0 = \text{shielding cutoff}$$

Proceed with SVA and discretize in x, s

Writing $u_j^n \approx u(s_n, x_j)$, use leap-frog in s and a 3-point rule in x:

$$\frac{u_j^{n+1} - u_j^{n-1}}{2\Delta s} = \frac{i}{2k}\Big(\frac{x_j + \rho}{\rho}\Big)^2 \Bigg[\frac{u_{j+1}^n - 2u_j^n + u_{j-1}^n}{\Delta x^2} + \frac{1}{x_j + \rho}\frac{u_{j+1}^n - u_{j-1}^n}{2\Delta x} + \left(\gamma_p^2 - \Big(\frac{k\rho}{x_j + \rho}\Big)^2\right) u_j^n - S(x_j)\Bigg] \; . \quad (3)$$

But this won't work if S is a line charge, as we assume in a first try:

$$S = \hat{S}_{Ep}(k, x) = \kappa(k, p)\delta(x) \; .$$

The remedy: make a change of dependent variable so that the effective source for the new variable v is regular:

$$u(x) = v(x) + \xi(x) \; , \quad \xi(x) = \kappa(1 - x/2\rho)x\theta(x) \; .$$

Effective source for $v(x) = u(x) - \xi(x)$

v satisfies the same wave equation as u, but with a smooth source instead of a delta function.

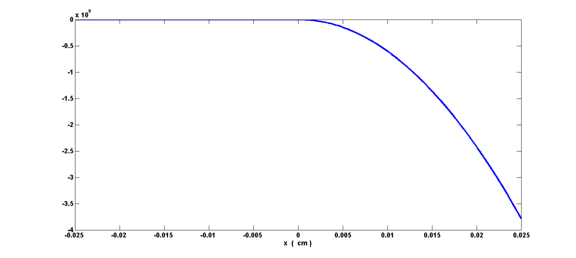

A similar change of variable can be done for a source of small but finite width, to make the effective source broader and smoother. Do that in a macroparticle simulation!

Enforcing boundary conditions on the side walls, $x = x_\pm(s)$

For constant cross section, $x_\pm$ =const., the conditions are

$$v_E(x_\pm) = -\xi_E(x_\pm) \ , \quad \partial_x v_H(x_\pm) = -\partial_x \xi_H(x_\pm) \ . \tag{4}$$

For variable cross section with walls at $x_\pm(s)$, the conditions are

$$\begin{aligned} & v_E(x_\pm(s)) = -\xi_E(x_\pm(s)) \ , \\ & \left[t_s(s)\partial_x u_H - \frac{t_x(s)}{1 + x/\rho}(iku_H + \partial_s u_H) \right]_{x = x_\pm(s)} = 0 \ , \end{aligned}$$

where (t_s, t_x) is the tangent vector to the relevant wall.

All boundary values can be expressed in terms of field values at interior mesh points $x_2, \cdots, x_{n-1}$ so that we evolve $n-2$ unknowns with $n-2$ linear differential equations.

Result of the simple algorithm in Eq.(3):

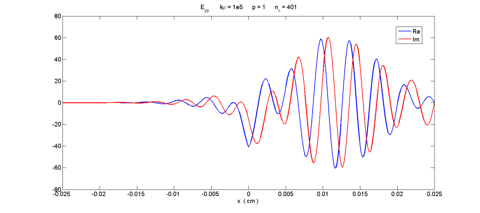

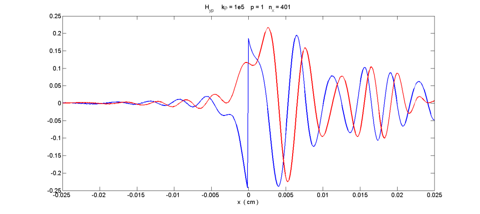

End of last bend in BC2, LCLS-II, 10μm bunch length. Initial condition: steady state solution in infinite straight pipe.

Method applied to resistive wall heating and wake fields

R. Warnock and D. Bizzozero, Phys. Rev. Accel. Beams **19**, 090705 (2016)

- Used 5-point rule (agrees with recent 3-point results).
- Found energy deposited in resistive walls by perturbative treatment of Poynting flux.
- Very fast computation of longitudinal wake field for short realistic bunch (LCLS-II, 10μm).

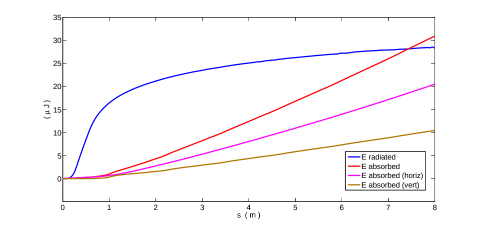

Figure: Energy radiated (blue) and absorbed (red) in bend and following straight (LCLS-II, BC2 final bend)

Avoiding the Courant-Friedrichs-Lewy (CFL) condition

Stability of the s-integration requires $\Delta s < \alpha k (\Delta x)^2$, where in our case $\alpha \approx 0.2$. This can mean 30000 s-steps in going through a bend, which seems a lot, but actually gives a much faster computation than previous methods.

A standard way to avoid the CFL condition is to invoke an implicit evolution algorithm, for instance the Crank-Nicolson or trapezoidal method:

$$\frac{1}{\Delta t}\left(u^{n+1} - u^{n}\right) = \frac{1}{2}\left(f^{n}(u_{xx}, u_{x}, u) + f^{n+1}(u_{xx}, u_{x}, u)\right)$$

When u_{xx} and u_x are given by a 3-point rule as in (3), we have a tridiagonal system to solve for u^{n+1} in terms of u^n.

The solution is fast and allows a much bigger Δs, say 300 steps in place of 30000. Cost per step not much larger.

Avoiding the slowly varying amplitude approximation

Could we restore the neglected u_{ss}, thus getting the exact Maxwell system? When using an explicit integrator, that leads to a gross instability.

At a recent seminar at LBNL, I saw a second time derivative in a so-called Crank-Nicolson scheme. See C. Benedetti *et al.*, Proc. ICAP 2012, THAA12.

In INF&RNO, the evolution equation for the laser envelope, Eq. 1, is discretized in time using a Crank-Nicholson scheme which reads

$$
\begin{aligned}
& - \frac{\hat{a}^{n+1} - 2\hat{a}^{n} + \hat{a}^{n-1}}{\Delta_\tau^2} \\
& + 2\left[i\frac{k_0}{k_p} + \frac{\partial}{\partial \xi}\right]\left(\frac{\hat{a}^{n+1} - \hat{a}^{n-1}}{2\Delta_\tau}\right) = \\
& - \nabla_\perp^2\left(\frac{\hat{a}^{n+1} + \hat{a}^{n-1}}{2}\right) + \frac{\delta^n}{\gamma^n_{\text{fluid}}}\frac{\hat{a}^{n+1} + \hat{a}^{n-1}}{2},
\end{aligned}
\tag{5}
$$

Would that be allowed in our somewhat similar equation ?

Beyond the SVA approximation with implicit integrator

After Benedetti *et al.* I tried the following (with F from (3)):

$$\frac{1}{(\Delta s)^2}\left(u^{n+1} - 2u^n + u^{n-1}\right) + \frac{2ik}{\Delta s}\left(u^{n+1} - u^n\right) =$$
$$\frac{1}{2}\left(F^n(u_{xx}, u_x, u) + F^{n+1}(u_{xx}, u_x, u)\right) .$$

This was found to be stable if $2k\Delta s \gg 1$, which can be achieved with the large Δs allowed by the implicit integrator.

This is true at least for the smooth vacuum chamber, in which case the computed u_{ss} is actually negligible (i.e., the SVA approximation is good, as is expected in a smooth chamber).

The next big question: will the integration still be stable for a corrugated chamber in which u_{ss} will not be negligible?

Summary and Outlook

- We have a fast and very simple way to compute fields of a bunch in a rectangular chamber of variable width, through any sequence of bends and straights.
- Since the calculation is the easier the higher the frequency, very short bunches can be treated.
- Promising for self-consistent macroparticle simulation with CSR and space charge in single-pass systems (bunch compressors, etc.). Field calculation and Fourier transformations a small part of the cost.
- Hope to develop the code with Chris Mayes as part of BMAD, with 3D charge/current.

New angles:

- Explore the full Maxwell system without SVA, using implicit integrator.
- Impose periodicity in s, study local resonances within a period.

Connection to stability theory of ODE's

We can put the equation with second derivative into first order form by defining $w = du/ds$, thus getting a first order system for (u, w). Apply the trapezoidal rule to that system.

A great feature of the trapezoidal rule is that it is A-stable after the definition of Dahlquist. An A-stable numerical integrator is one that gives the correct asymptote of zero when applied to the trivial equation $du/ds = \lambda u$, $\mathrm{Re}\ \lambda < 0$, for any step size Δs. My guess is that this good property of the trapezoidal rule will lead to a stable solution of our complete Maxwell system cast in first order form, even with boundary conditions for a corrugated wall.

Some New Methods for Numerical Solution of Nonlinear Equations, with Suggested Applications in S Matrix Theory+)

Robert L. Warnock*)

Physikalisches Institut der Universität Bonn

and

Department of Physics, Imperial College, London S. W. 7

Lectures at the

Physikalisches Institut der Universität Bonn

February, 1972

A b s t r a c t

This is an introduction to some new methods for numerical solution of nonlinear equations, written from the point of view of a high energy physicist. The methods are based on imbedding the original nonlinear operator in a family of operators depending on a parameter. The original problem is solved by means of a differential equation, in which the parameter appears as the independent variable. This is a general and effective technique, which appears to be quite suitable for nonlinear problems in scattering theory. Examples of such problems are presented.

Zuppa Arcidossana

By Mark Bittman | **YIELD 4 servings** | **TIME 25 minutes**

INGREDIENTS

2 tablespoons olive oil

¼ pound sweet Italian sausage, removed from casings

1 cup 1/2-inch-diced carrots

1 large onion, chopped

3 or 4 cloves garlic, chopped

Salt

black pepper

1 cup stale bread (use coarse, country-style bread), cut in 1/2-inch cubes

½ pound spinach, trimmed, washed and roughly chopped

¼ to ½ cup ricotta salata, cut in 1/2-inch cubes (feta may be substituted)

¼ cup freshly chopped parsley, optional

PREPARATION

Step 1

Put oil in a large pot or deep skillet and brown sausage over medium-low heat, stirring occasionally. When sausage is cooked through and leaving brown bits in pan, add carrots, onion and garlic, and continue to cook until vegetables begin to soften and brown, about 10 minutes. Sprinkle with salt and pepper.

Step 2

Add bread to pan and stir for a minute or 2; add spinach and continue cooking just until it wilts, a couple of minutes.

Step 3

Add about 2 cups water and stir to loosen any remaining brown bits from pan. This is more of a stew than a soup, but there should be some broth, so add another cup of water if necessary. When broth is consistency of thin gravy, ladle stew into serving bowls and top with cheese and some freshly chopped parsley if you have it. Serve immediately.

PRIVATE NOTES

Leave a Private Note on this recipe and see it here.

Featured in: A Soup Only Tuscany Could Make (http://www.nytimes.com/2009/04/29/dining/29mini.html).